

Computational models of hair cell bundle mechanics: II. Simplified bundle models

John Cotton, Wally Grant *

*Department of Engineering Science and Mechanics and School of Biomedical Engineering and Sciences,
Virginia Polytechnic Institute and State University, Mail Code 0219, Blacksburg, VA 24061, USA*

Received 21 April 2003; accepted 21 June 2004
Available online 1 September 2004

Abstract

Simplified versions of hair cell bundles are mechanically modeled. The influence of various geometric and material combinations on bundle stiffness, link tensions and deformation shape are examined. Three models are analyzed within this paper: two stereocilia connected by one link, two stereocilia connected by a biologically realistic set of links, and a column of stereocilia connected by realistic links. Stereocilia are modeled using a distributed parameter model [J. Biomech. Eng. 122, 44]. Some fundamental rules for linking bundles emerge from these tests: (1) Links must have a threshold stiffness value for the bundle to deform as a whole. Beyond this value, the stereocilia are perfectly linked and variations in link stiffness do not significantly effect the bundle stiffness or link tension. (2) Decreasing the relative heights of successive stereocilia may increase link tension while decreasing bundle stiffness. (3) When lateral links exist, the top most lateral links carry the majority of tension. Lower links in single column model appear mechanically insignificant. (4) Extending the length of the bundle in a column does not increase the stiffness once the column reaches a certain length. © 2004 Elsevier B.V. All rights reserved.

Keywords: Hair cell bundle; Mechanical model; Bundle stiffness; Distributed parameter bundle model

1. Introduction

Hair cell bundles consist of many cilia interconnected by fine link structures. Many geometric variations are seen in the organization of these cilia and links. These geometric variations within bundles are well documented (Lewis et al., 1985) and it is hypothesized that they are a source of functional variations. Presented here is a theoretical analysis of the effects of structural and material variations within the general structure of hair cell bundles.

This paper is the second of three addressing this topic. Part I discusses the mechanics of an individual stereocilium (Cotton and Grant, 2004). Part II (this paper) discusses some fundamental principles of bundle behavior.

Herein, individual stereocilia are connected together with links in simplified models. The behavior of these models is investigated to identify some fundamental physical rules about linking stereocilia. Part III presents a study of real three-dimensional bundles (Silver et al., 2004).

Three models will be investigated in this paper. They are two cilia connected by a single link (Fig. 1, Model A), two cilia connected by several links distributed and oriented to reflect biologic reality (Fig. 1, Model B), and a column of stereocilia connected by biologically realistic links (Fig. 1, Model C). A single force applied at the top of the tallest stereocilium provides deformation for all models.

We will perform parametric studies on these simplified structures, varying stereocilia height, link stiffness, link distributions, and column lengths. Output parameters studied will include overall assembly (i.e., bundle) stiffness and link tensions.

* Corresponding author. Tel.: +540-231-4573; fax: +540-231-4574.
E-mail address: jgrant@vt.edu (W. Grant).

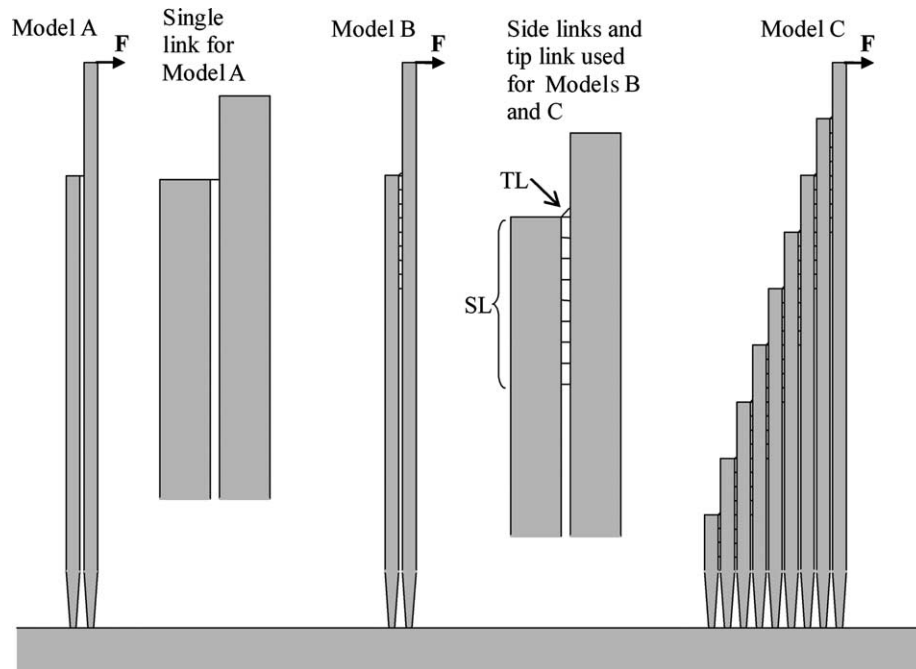


Fig. 1. Models presented in this paper are: Model A. Two cilia connected by one link. Model B. Two cilia connected by tip link and multiple shaft links. Model C. A column of cilia connected by tip links and multiple shaft links. These figures are drawn to an approximate relative scale. All models are forced by a single point force, F , located at the tip of the tallest stereocilium in each model. Links are classified as tip links, TL and shaft links, SL, as labeled in Model B.

2. Methods

2.1. Bundle mechanics and non-dimensional parameters

Earlier work in this series established the mechanics of a single stereocilium, we continue to use the preceding model for the single stereocilium. In this model, cilium mechanics are well described by Timoshenko beam theory (Reddy, 1993; Cotton, 1998), in which the cilium deforms both from bending and shear. It is concluded that the shear modulus for the stereocilium is much lower than it would be for an isotropic material, making shear deformation relevant for many bundle geometries despite the high aspect ratio of the stereocilia. In addition, stereocilia taper at their bases resulting in a reduced cross sectional area and significant deformation in the form of bending that takes place in this region.

Cilium stiffness, k_s , was defined for a single (unlinked) cilium as the force, F , applied at the tip divided by the tip deflection, x , or

$$k_s = \frac{F}{x}. \quad (1)$$

Similarly, when stereocilia are connected into an bundle, the bundle stiffness, k_b , is the applied force applied to the tallest stereocilium divided by the tip deflection of the tallest stereocilium

$$k_b = \frac{F}{x}. \quad (2)$$

Despite the fact that none of the assembled stereocilia in this paper are biologically realistic bundles, we will use the term bundle stiffness to describe the stiffness of these assemblies of stereocilia in a column.

The links were modeled as two-force members or structures that resist deformation along their long axes. They can be thought of as a spring with equal and opposite forces applied at each end, and the force is acting along the axis of the spring. The formula that relates the applied force f , to deflection δ can be found in strength of materials textbooks (Beer and Johnston, 2001)

$$f = \frac{EA}{l} \delta, \quad (3)$$

where E is the Young's modulus of the link, A is the link's cross sectional area (assumed round) and l is the length of the link. This applied force f is equal to the tension in the link. For comparison to stiffness already introduced, the stiffness of the links, k_ℓ , will be determined from Eq. (3) by dividing the link tension f by the elongation δ

$$k_\ell = \frac{f}{\delta} = \frac{EA}{l}. \quad (4)$$

The applied force in all these models will be placed at the top of the tallest stereocilium. The magnitude is consistently held at 10 pN, although most of the models are linear in their response and therefore the force magnitude is not relevant.

Non-dimensionalization will help draw the most general conclusions about bundle mechanics. Results were non-dimensionalized using the following variables for force, stereocilia height, and stiffness

$$\bar{f} = \frac{f}{F}, \quad \bar{l}_i = \frac{l_i}{l_\ell}, \quad \bar{k}_\ell = \frac{k_\ell}{k_s}, \quad \bar{k}_b = \frac{k_b}{k_s}, \quad (5)$$

where l_1 is height of the tallest (forced) stereocilium, F is the applied (external) force, l_i are successive stereocilia heights, k_s is the stiffness of the tallest stereocilium, and k_b is the stiffness of the entire bundle. In addition, the coordinate height and bundle deflection were non-dimensionalized

$$\bar{y} = \frac{y}{l_1}, \quad \bar{x} = \frac{x}{l_1}. \quad (6)$$

In this process all non-dimensional stiffness is compared to the stiffness of the tallest stereocilia, all distances are compared to the tallest stereocilia height, and the forces are all compared to the applied bundle force. For comparisons of bundle model stiffness, a single stereocilium 10 μm tall under a point load of 10 pN was simulated to determine the stereocilia stiffness, k_s , for non-dimensionalization.

The results of the analysis to follow are presented in terms of these non-dimensional parameters and variables. Bundle physical variables used to establish a start-

ing value for these non-dimensional quantities are presented in Table 1. The values in this table reflect the general ranges of these quantities and should not be thought of as established values and are not intended to be precise. The range of non-dimensional parameters and variables are described with specific models below. Also included in Table 1 are stiffness values for the tallest stereocilium and the standard tip and side link. Stereocilia dimensions are realistic values for vestibular bundles. The stereocilia Young’s Modulus represents that of actin fibers (Gittes et al., 1993). The ciliary shear modulus represents a current best value, from previous work (Cotton and Grant, 1997, 2000; and unpublished tests).

2.2. Bundle models

The first model, Model A (Fig. 1) was two cilia connected by a single link, located at the top of the shorter cilia, extending horizontal to the taller cilium. It was run for two tests. The first held the second stereocilium height at a constant 80% the height of the first ($l_2/l_1=0.8$). This configuration was tested for variations in the non-dimensional link stiffness (k_ℓ/k_s). Overall bundle stiffness as well as the link tension was calculated for each case. Also generated were deformation profiles for several of the cases.

Table 1
Properties use to establish initial non-dimensional parameter values

Property	Value	Source
<i>Stereocilia</i>		
<u>Geometric properties</u>		
Shaft diameter	0.24 μm	Measured from TEM
Root diameter	0.12 μm	Measured from TEM
Taper height	1 μm	Measured from TEM
Height of tallest stereo.	10 μm	Measured from LM and SEM
<u>Material properties</u>		
Young’s modulus, E	$3 \times 10^9 \text{ N/m}^2$	Gittes et al. (1993)
Shear modulus, G	$1 \times 10^6 \text{ N/m}^2$	Cotton and Grant (2000)
Stiffness of tallest	$0.651 \times 10^{-3} \text{ N/m}$	Calculated from properties
<i>Tip links</i>		
Young’s modulus, E	$3 \times 10^6 \text{ N/m}^2$	A minimum value
Diameter	10 nm	Kachar et al. (2000), Tsuprun and Santi (2000)
Length	57 nm	Calculated from geometry
Angle of application	45°	Estimated from TEM and SEM
Stiffness	$3.4 \times 10^{-3} \text{ N/m}$	Calculated from properties
<i>Side links</i>		
Young’s modulus, E	3×10^6 or $4.1 \times 10^7 \text{ N/m}^2$	Sufficient to hold stereocilia together
Diameter	9 nm	Duncan and Grant (1998)
Length	40 nm	Measured from TEM
No. connecting two stereocilia	9	Estimated
Spacing between links	0.25 μm	Estimated
Stiffness	4.8×10^{-3} or $6.5 \times 10^{-2} \text{ N/m}$	Calculated from properties
<i>Applied force</i>		
Force	10 pN	

The second test with model A varied the height of the second stereocilium from 100% to 10% of the height of the first. These tests were run with reasonably stiff links as determined from the results of the first test. The significance of this will be discussed with the results below. This value was chosen to be $k_\ell/k_s=100$, and was achieved by setting the link's Young's Modulus to $4.1 \times 10^7 \text{ N/m}^2$. Bundle stiffness and link tension was calculated for these cases.

Model B (Fig. 1) connects two stereocilia with two realistic link types: the side links, which are numerous and are parallel to the apical surface, and the tip link, of which there is one which extends at an angle relative the apical surface (Goodyear and Richardson, 1994). Side link stiffness is unknown, hence it will be varied in parametric studies. Each side link was assumed to have a length equal to the side-to-side intercilary spacing of 40 nm. Variations in link stiffness can be related to the components that make up this stiffness value: Young's modulus of the link material, link diameter, and the total number of links at each location. There may be more than one fiber connecting the stereocilia at each height, however, in this model only a single fiber will be used at a given height. The effects of multiple fibers at a given height can be thought of as being lumped into this single fiber.

Variations in tip link stiffness are addressed in a similar manner. A base value of link stiffness of $3.4 \times 10^{-3} \text{ N/m}$ (Eq. (4)) was calculated. This value reflects a Young's modulus of $2.4 \times 10^6 \text{ N/m}^2$, which is above the range of values from elastin ($E_{\text{elastin}} = 6 \times 10^5 \text{ N/m}^2$), and in the range of values calculated indirectly from experimental work by Howard and Hudspeth ($4 \times 10^6 \text{ N/m}^2$), and low compared to recent estimates ($1 \times 10^7 \text{ N/m}^2$, used in No. III in this series). It also reflects a diameter of 10 nm (range 9–12 nm (Kachar et al., 2000; Tsuprun and Santi, 2000)) and a length of 57 nm, based upon the geometry of the model. This length is calculated from a horizontal intercilary spacing used here of 40 nm (Peterson et al., 1995; Howard and Ashmore, 1986; and measured from TEM) and a tip link that extends at a 45° angle to the horizontal from the cilia edge (i.e., $40 \text{ nm} = 57 \sin(45^\circ)$). The length could be up to three times this value (Kachar et al., 2000). While these values are all in accepted ranges, there is a degree of uncertainty in all, however, the resulting stiffness is accurate within an order of magnitude.

The height of the second stereocilium was set at 80% of the first stereocilium. We calculated the stiffness of the assembly for ranges of side link stiffness. Tip link stiffness was held constant at standard values given in Table 1. We also calculated the tension in the tip links and side links.

Model C (Fig. 1) uses the same link structure as the B model, but has more than two cilia in a straight line or column. Columns of two to nine cilia were simulated.

Successive stereocilia decrease in height linearly, with the tallest cilium given a height of 10 μm , the second 9 μm , the third 8 μm , and on to the ninth cilium which has a height of 2 μm . A linear drop of height was used because it is the simplest and most common. In all other measures, the stereocilia are identical. The assembly stiffness was calculated, as well as the tension in the tip links. Also presented here will be the tension in the uppermost side link.

All modeling was performed by a custom-written code that performs a finite element analysis (FEA) on the bundles. This program is based on the structural models of stereocilia from the first manuscript in this series, and links discussed here. Details of this program are reported in Cotton and Grant, 2000).

3. Results and discussion

The tip of the single unlinked stereocilium deflected 15.4 nm under the 10 pN applied load, giving the single cilium a stiffness of $k_s = 651 \text{ pN}/\mu\text{m}$ ($6.51 \times 10^{-4} \text{ N/m}$). This value is in the range of reported values from other researchers (Szymko et al., 1992.)

3.1. Model A

Model A (the two stereocilia model with single link) was tested for a variety of link stiffness values; variations in stiffness and link tension are shown in Fig. 2. For small link stiffness values where, $\bar{k}_\ell = k_\ell/k_s < 0.1$, the bundle has the same stiffness as a single stereocilium. The link is too compliant and negligible tension is carried in the link; thus the second cilium neither deflects nor contributes to bundle stiffness. Small increases in link stiffness in this range have little effect on link tension or bundle stiffness. As link stiffness is increased into the next regime where $0.1 < \bar{k}_\ell = k_\ell/k_s < 10$, both bundle stiffness and link tension are strongly dependent on link stiffness. Small variations of link stiffness in this range will effect the bundle mechanics significantly,

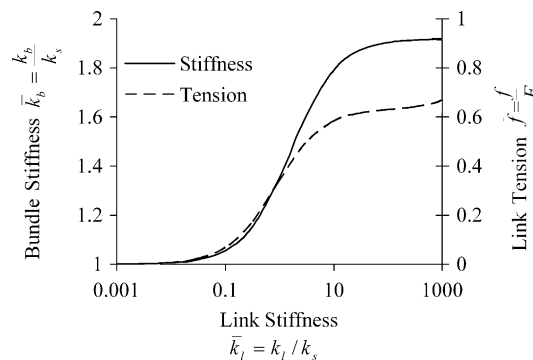


Fig. 2. For model A (Fig. 1), the bundle stiffness and link tension as a function of link stiffness.

and precise values of link characteristics would be necessary to model bundles. When $\bar{k}_\ell = k_\ell/k_s > 10$, a threshold value is reached. The link has become stiff enough that both bundle stiffness and link tension do not depend on the link properties, but on the stiffness of the two component cilia alone. The link behaves as a rigid member and its specific properties are unimportant to the bundle behavior. In this situation, the bundle stiffness reaches a maximum value roughly equal to twice that of a single stereocilium.

Fig. 3 contains profiles of model A (the two stereocilium model) for different link stiffness values. The first profile, with link stiffness $\bar{k}_\ell = k_\ell/k_s = 10^{-3}$, shows that the taller stereocilium deforms while the shorter cilium is unaffected. This is clearly non-biologic. The second profile, with link stiffness $\bar{k}_\ell = k_\ell/k_s = 10^0$, shows the second cilium deforming but at a much smaller magnitude than the first. This is also non-biologic. The spread between stereocilia has been termed splay, and has not been seen experimentally by some (Corey et al., 1989), while other researchers have seen very small amounts of splay (Duncan et al., 1995). Large splay amounts are not reported. The third profile with link stiffness $\bar{k}_\ell = k_\ell/k_s = 10^2$, shows the bundle tightly linked together, deforming in unison, with imperceptible splay, and this is the way bundles are observed to deform (Flock et al., 1977; Hudspeth, 1983; Corey et al., 1989). Thus, for cilia to deform in unison, link stiffness must be sufficient to deform the second (shorter) stereocilium, and in general, any successive stereocilia. Referring back to Fig. 2, the link stiffness must be in the high plateau region which corresponds to link stiffness values of $\bar{k}_\ell = k_\ell/k_s > 10$. This also implies accurate descriptions of link geometries and good estimates of material properties are unnecessary for accurate modeling of bundle mechanical behavior.

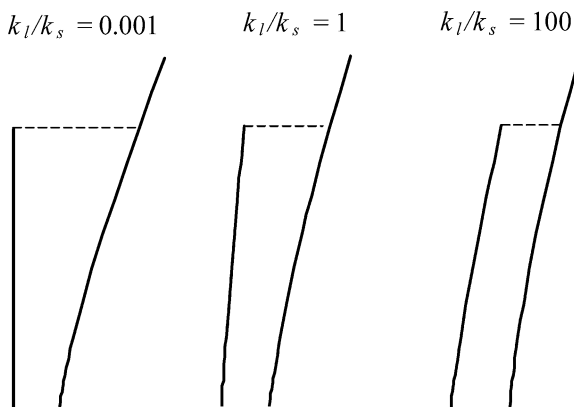


Fig. 3. Profiles of Model A for two stereocilium and one link in model A (Fig. 1). Links are shown as dashed lines. The three regimes for bundle behavior are shown for various values of link stiffness ratio. Note: the spacing between cilia is exaggerated to illustrate the effect.

For the final test with model A, the height of the second, shorter stereocilium was varied. Stiff links were used ($\bar{k}_\ell = k_\ell/k_s > 10^2$), corresponding to the high plateau region in Fig. 2) to make sure the bundle was tightly coupled. Results of these tests are shown in Fig. 4. Decreasing the height of the shorter stereocilium reduces the stiffness of the bundle assembly. This is because the second cilium does not support the taller cilium as high along its shaft, making it a less ideal brace. On the other hand, the taller cilium acts as a lever arm, magnifying the tension in the link more as the link is placed lower along the shaft. This results in higher link tensions if successive stereocilia are significantly shorter. The link tension may even be greater than the applied force when successive stereocilia are low enough, which for the scenario presented here is $\bar{l}_2 = l_2/l_1 < 0.5$.

3.2. Model B

Model B replaces the single link of the model A with a more complete set of links. First shown in Fig. 5 is how the side link tension varies due to the side link stiffness. The side links nearest the top (link 1 and 2) contain significant tensions whereas the lower links have diminishing tensions. The lowest side links modeled do not carry any tension for realistically stiff side link values of $\bar{k}_\ell = k_\ell/k_s = 10$. This suggests why side links are concentrated near the tips of the cilia. It also suggests the insignificance of including lower links in mechanical bundle modeling.

How bundle stiffness increases with varying the side links stiffness is shown in Fig. 6. This is consistent with Fig. 2 for the first model. By adding the additional links, bundle stiffness saturates at a maximum value of nearly twice the single cilium stiffness when the side link stiff-

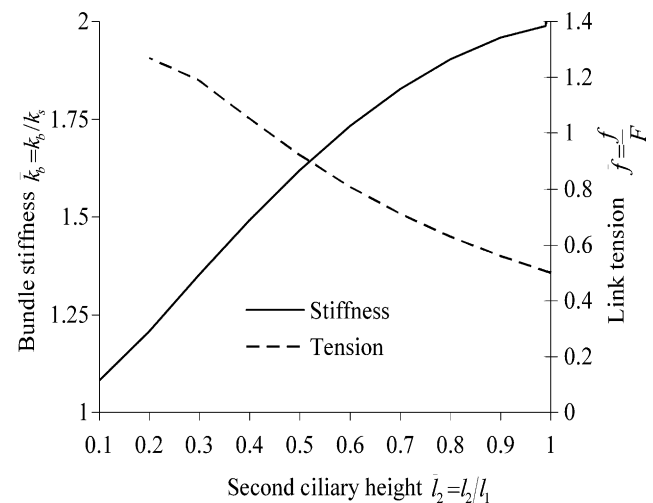


Fig. 4. For Model A, the two cilium-one link model (Fig. 1), results if the link is very stiff ($k_\ell/k_s = 100$) and the height of the second stereocilium is varied.

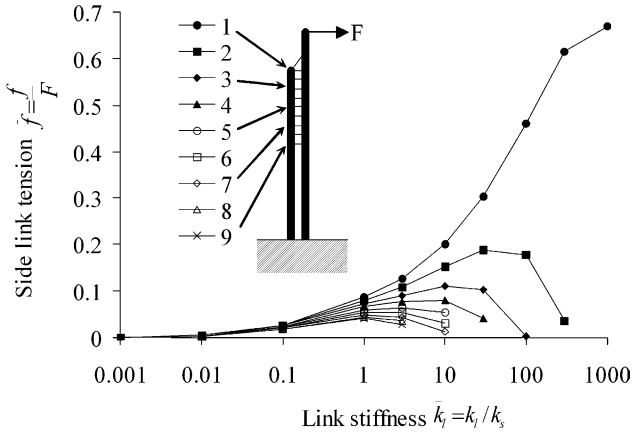


Fig. 5. For Model B, two cilia and several link model (Fig. 1), the tension in side links (numbered from the top down) as a function of link stiffness ratio. Note. Tip links are not included in the plot. For link stiffness values that are realistic ($k_l/k_s \geq 10$), the lower links have tensions that are very low. The lowest values are terminated when the tensions become small or slack (no provision is made for these links to carry a compressive load).

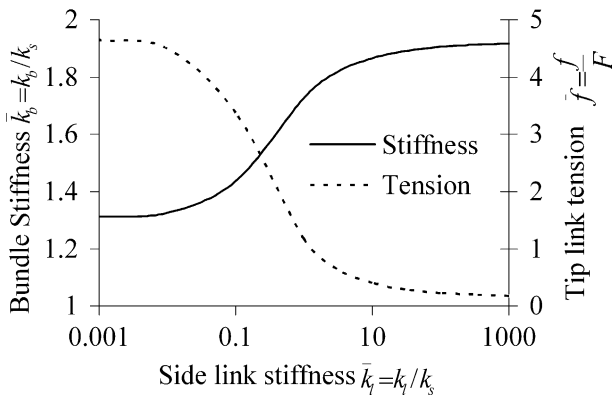


Fig. 6. For Model B (Fig. 1), the tension in the tip link and the assembly stiffness as a function of the side link stiffness.

ness is approximately 3 times the cilium stiffness ($\bar{k}_l = k_l/k_s = 3$). The tension in the tip link decreases however with increased side link stiffness. Fig. 6 presents how the tip link tension drops to a nearly constant value when side links are stiff. This is because the mechanical linking of stereocilia is being achieved by the side links, leaving the tip link to deform due to geometry alone. In these cases, the tip link tension is small when compared to side link tensions (Fig. 5). This also suggests a closer examination of side link structures for all hair cells, if tip links are to have significant mechanical influence on bundle stiffness.

3.3. Model C

The third model adds additional stereocilia, extending back in a single column to the second model. As the column length grew, so did the assembly stiffness (Fig. 7). However, the stiffness grew the most when the

second cilium was added. With each successive cilium, the increase in stiffness is less than the previous. By the addition of the seventh cilium, very little increase in bundle stiffness is seen.

Also shown are the tensions in both tip links (Fig. 8) and the topmost side link (Fig. 9) as the column length

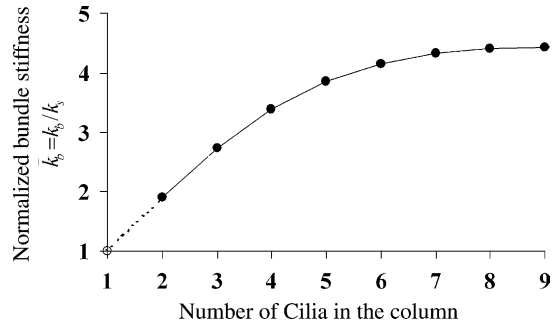


Fig. 7. For Model C, a column of cilia (Fig. 1), the bundle stiffness increase as cilia are added.

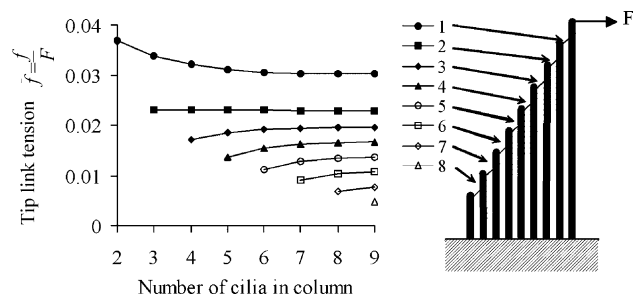


Fig. 8. For Model C (Fig. 1), the tension in tip links as the number of cilia in the column increases. Links are numbered such that link 1 connects the tallest stereocilium to the second, and each successively numbered link is further away from the tallest cilium in the column. The top curve represents the tension in tip link 1 as successive cilia are added to the column. The next curve below the top curve represents the tension in tip link 2 as successive cilia are added, and successive additions are shown as one moves down the family of curves. When the 9th cilium is added (8th tip link) the tension in that link is represented as a single point.

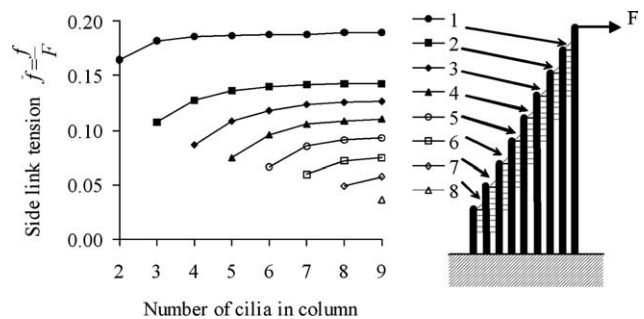


Fig. 9. For Model C (Fig. 1), tension in side links as the number of cilia in the column is increased (cilia are added to the column). Links are numbered such that link 1 connects the tallest stereocilium to the second, and each successively numbered link is further away from the tallest cilium in the column.

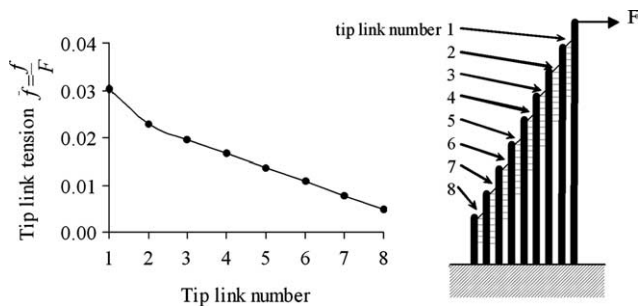


Fig. 10. Tension in tip links for a 9 cilia column, model C (Fig. 1). Links are numbered such that link 1 connects the tallest stereocilium to the second, and each successively numbered link is further away from the tallest cilium in the column.

grew. Interestingly, having additional cilia does not seem to effect the tensions in any but the closest one or two stereocilia. Finally, the tensions in all tip links are presented for a column of nine cilia (Fig. 10). This shows that the tip link tension will decrease as the distance from the tallest cilium increases. The drop in tension though, is moderate enough so that the tension in the last link is still significant.

4. Conclusions

In summary, by investigating overall bundle deformation of a single column of cilia, the following conclusions could be drawn. The side links must be sufficiently stiff to prevent splay of the stereocilia and transfer load so that the complete bundle deforms essentially in unison. Once this threshold stiffness is reached, however, the actual side link stiffness is not critical to determining bundle stiffness or tip link tension. Earlier work (Pickles, 1993) used a different model to reach similar conclusions regarding relative stiffness of bundle components.

Link tension increases with decreased height of successive stereocilia, while bundle stiffness decreases. This suggests variations in height within a column would allow bundles, via their geometric variation, to reach exact link tensions at different deflections and/or applied loads. A case study of the effect of height changes is included in Peterson et al. (1995).

Adding extra stereocilia in a column increases bundle stiffness to a degree, however, after a certain point they will have little effect on stiffness. Tip link tensions are still significant, but decreased as the distance from the tallest stereocilium increases.

The techniques presented here highlight several roles for mechanical modeling. It can play a role in determining structural dimensions as well as identifying component material properties. It can indicate why a certain structure follows a certain form. Finally, it can indicate

which portions of the structure are robust and which are sensitive to small changes.

Acknowledgements

This work was supported by the National Institute of Health R01 DC05063, and the National Science Foundation IBN-9724123.

References

- Beer, F.P., Johnston, E.R., 2001. *Mechanics of Materials*, third ed. McGraw-Hill, New York.
- Corey, D.P., Huang, P.L., Assad, J.A., 1989. Hair cell stereocilia bend at the bases and touch at their tips. *Soc. Neurosci. Abs.* 15, 208.
- Cotton, J.R., 1998. *Mechanical Models of Vestibular Hair Cell Bundles*. Ph.D. Dissertation, Virginia Polytechnic Institute and State University, Blacksburg, VA.
- Cotton, J.R., Grant, J.W., 1997. Analytic and finite element analysis of stereocilia-link systems: using deformation modes to infer hair cell bundle properties. Abstracts No. 157; Association for Research in Otolaryngology, St. Petersburg Beach, Florida.
- Cotton, J.R., Grant, J.W., 2000. A finite element method for mechanical response of hair cell ciliary bundles. *J. Biomechanical Engr.* 122, 44–50.
- Cotton, J., Grant, W., 2004. Computational models of hair cell bundle mechanics: I. Single stereocilium. *Hear. Res.*, this issue.
- Duncan, R.K., Grant, J.W., 1998. A finite element model of inner ear hair bundle micromechanics. *Hear. Res.* 104, 15–26.
- Duncan, R.K., Hernandez, H.N., Saunders, J.C., 1995. Relative stereocilia motion of chick cochlear hair cells during high-frequency water-jet stimulation. *Audit. Neurosci.* 1, 321–329.
- Flock, A., Flock, B., Murray, E., 1977. Studies on the sensory hairs of receptor cells in the inner ear. *Acta Otolaryngol.* 83, 85–91.
- Gittes, F., Mickey, B., Nettleton, J., Howard, J., 1993. Flexural rigidity of microtubules and actin filaments measured from thermal fluctuation in shape. *J. Cell Biol.* 120, 923–924.
- Goodyear, R., Richardson, G., 1994. Differential glycosylation of auditory and vestibular hair bundle proteins revealed by peanut agglutinin. *J. Compar. Neurol.* 345, 267–278.
- Howard, J., Ashmore, J.F., 1986. Stiffness of sensory hair bundles in the sacculus of the frog. *Hear. Res.* 23, 93–104.
- Hudspeth, 1983. The hair cell of the inner ear. *Sci. Am.* 248, 54–64.
- Kachar, B., Parakkal, M., Kurc, M., Zhao, Y.D., Gillespi, P.G., 2000. High-resolution structure of hair-cell tip links. *PNAS* 97 (24).
- Lewis, E.R., Leverenz, E.L., Bialek, W.S., 1985. *The Vertebrate Inner Ear*. CRC Press, Boca Raton.
- Peterson, E.H., Cotton, J.R., Grant, J.W., 1995. Structural variation in ciliary bundles of the posterior semicircular canal: quantitative anatomy and computational analysis. *Ann. N.Y. Acad. Sci.* 781, 85–102.
- Pickles, J.O., 1993. A model for the mechanics of the stereociliar bundle on acousticolateral hair cells. *Hear. Res.* 68, 159–172.
- Reddy, J.N., 1993. *Finite element method*, second ed. McGraw-Hill, New York.
- Silber, J., Cotton, C., Nam, J.-H., Peterson, E.H., Grant, W., 2004. Computational models of hair cell bundle mechanics: III. 3-D utricular bundles. *Hear. Res.*, this issue.
- Szymko, Y.P., Dimitri, P., Saunders, J., 1992. Stiffness of hair bundles in chick cochlea. *Hear. Res.* 59, 241–249.
- Tsuprun, V., Santi, P., 2000. Helical structure of hair cell stereocilia tip links in the chinchilla cochlea. *JARO* 01, 224–231.